INTERNATIONAL JOURNAL OF INTEGRATED ENGINEERING
ISSN: 2229-838X e-ISSN: 2600-7916

IJIE

Vol. 16 No. 6 (2024) 100-110
https://publisher.uthm.edu.my/ojs/index.php/ijie

Comparative Analysis of Modular Pin-Fin Heat Sink Performance: Influence of Geometric Variation on Heat Transfer Characteristics

Devia Gahana Cindi Alfian[1]*, Dicky Januarizky Silitonga[1], Muhammad Al Fajri Ramadhan[1], Ihsan Naufal Ridhwan[1], Rionaldi Prasetyo Utomo[1], I Made Rudiarta[1]

[1] *Department of Mechanical Engineering, Faculty of Industrial Technology, Institut Teknologi Sumatera, South Lampung, 35365, INDONESIA*

*Corresponding Author: devia.gahana@ms.itera.ac.id
DOI: https://doi.org/10.30880/ijie.2024.16.06.010

Article Info

Received: 1 February 2024
Accepted: 11 July 2024
Available online: 9 October 2024

Keywords

Heatsink, modular pin-fin, geometric, forced convection, convective heat transfer

Abstract

The advancement of digital technology in the age of Industrial Revolution 4.0 has driven other engineering sectors to keep up with the progressive demand for high-performance computing and electronics. Thermal management plays a critical role in maintaining the performance of electronic devices by keeping the system temperature at an optimal level and preventing overheating. A heat dissipation device widely employed in computing and other electronic systems' heat management is a fin-type heat sink, owing to its robust and simple design. In this work, the authors evaluated heat sinks of different pin-fin cross-sectional geometry, arranged in a staggered configuration, in terms of heat transfer characteristics under forced convection. Three basic geometries were chosen on the grounds of manufacturing easiness and market availability: circular, square, and hexagonal. All the tested geometries had approximately the same hydraulic diameter. Therefore, the results could be compared to each other. The investigation revealed that the square cross-section induced an excellent convection coefficient, hence higher heat dissipation, compared to the counterparts. The tradeoff between heat transfer performance and size-related parameters, such as surface area and material volume, is also discussed in this paper.

1. Introduction

The use of computers and electronic devices is continuously increasing due to the large number of work activities requiring high-performance electronic computing processes. In accordance with the market demands, the performance of electronic devices needs to be improved [1]. One of the significant aspects that can be fine-tuned to optimize the performance of electronic devices is in the sector of temperature control [2]. An electronic device generates heat during its operation, which has to be released to the environment to prevent overheating that may lead to malfunctions [3]. Although heat is a natural consequence of electronic device operation, excessive heating can slow down the system and induce damage to components. Therefore, it is mandatory to keep the temperature low to prevent adverse effects [4]. By maintaining the ideal operating temperature, the device will be able to deliver the performance level expected by the user [5].

The temperature stability in electronic devices can be maintained in various ways [6]. To dissipate the heat, one method is to utilize heat sinks in conjunction with a particular working fluid, using active and passive methods

[7]. Passive methods have the advantage of a cost-effective strategy, but it also has the disadvantage of a high initial cost for fluid pumping [8]. Although having a negligible running cost, passive cooling suffers from its low effectiveness [9]. As a result, active methods employing forced convection are commonly engaged to enhance heat transfer, hence the cooling effect [10]. That being said, compared to passive methods, forced convection cooling methods with air or liquid are far more effective solutions [11]. The active cooling concepts based on forced convection may be implemented in many forms, such as heat sinks under the external flow of fluid or cooling blocks where the heat is evacuated by the internal flow [12].

Installing a heat sink on a heat-generating component is the most widely implemented method to enhance heat transfer [13]. The heat sink serves as a heat exchanger that drains heat from electronic components to their surroundings. In a heat sink, the heat flows from a surface in contact with a heat-generating object to the other surface that is exposed to the environment or working fluid [14]. Increasing convection heat transfer can be done by expanding the area or heat transfer area through the use of an extended surface, such as fins of diverse features [15]. Apart from the area, heat transfer can also be influenced by geometric shapes, flow conditions, and fluid properties [16].

In this work, the use of the extended surface in heat sink applications is demonstrated through the application of various shapes of fins. The geometric features affect heat transfer properties by increasing the heat surface area [17] and by altering the flow of fluid. Fin-equipped heat sinks generally use air as a heat transfer medium [18]. Besides geometric features, heat sinks' performance can also be tuned up by selecting materials with high thermal conductivity values [19]. This aims to minimize the temperature difference between the prime and extended surfaces. Past research on several common engineering metals shows that, within the same Reynolds regime, the highest heat transfer rates of a heat sink can be achieved by using copper, followed by brass, aluminum, and finally steel [20].

Various types of fins are usually used, ranging from rectangular, cylindrical, annular, tapered, or pin shapes to a combination of different geometries with regular spacing in staggered and aligned arrangements [21]. The pin fin is a solid-shaped element that is mounted perpendicular to the wall of the heat exchanger apparatus, with the coolant flowing in a stream that is transverse to the wall of the heat-affected surface. The fins extrude from the surface that undergoes heating, thus providing an additional area for heat dissipation. In addition, fins induce turbulent flow mixing that is favorable for heat transfer.

Pin fin types can be classified based on parameters such as shape, height, diameter, height-diameter ratio (H/D), and so on [22]. Pin fins with a height-diameter ratio (H/D) between 0.5-4 are categorized as short pin fins, while a height-diameter ratio greater than four can be classified as long pin fins [23]. A large value of the height-diameter ratio is closely related to the high heat transfer coefficient. In addition, the pin fin arrangement also affects the heat transfer amount [24]. The study found that mass flow rate, S_x/D, and S_y/D are among the parameters that affect pin-fin heat sink performance [25].

Furthermore, staggered arrangement results in better heat transfer enhancement compared to the aligned arrangement [26]. The heat transfer rate at a given temperature can be amplified by raising the average heat transfer coefficient, expanding the surface area, or both. Also, faster heat rejection can be done by increasing the velocity of the fluid flowing around the hot surface through forced convection and changing its geometric configuration [27].

Heat transfer characteristics in pin-fin systems are important factors pertaining to the advancement of cooling system performance in various engineering applications [28]. This work examines the heat transfer characteristics of several pin fin geometries with a staggered arrangement. The goal is to gain an understanding of how different pin geometries perform in evacuating heat, identify which geometry outperforms the others, and recognize any tradeoffs that may accompany the performance profile. In this study, the heat sink specimens are varied in terms of pins' shape or geometry while keeping the hydraulic diameter equal for all of them. Geometries chosen for this project are those commonly manufactured and marketed, i.e., square, hexagonal and circular.

As a unique feature of this work, the pin-fin heat sink specimen is assembled modularly, enabling changes of pins or their arrangements as necessary. In this investigation, pins are configured in a staggered configuration on the heat sink plate, which applies to the specimens. Furthermore, tests were also carried out at varying air speeds and heating power. The result of this investigation will become a basis for further research involving an intricate structure of pin-fins to optimize heat dissipation.

2. Experiment and Analytical Approach

2.1 Experimental Setup

The experiment was conducted by mounting a heat sink specimen in a forced convection apparatus, TecQuipment TD1005. The apparatus features a vertical duct with a rectangular cross-section of 128 mm x 75 mm and a length of 850 mm. The duct's walls were of steel plate except for the front side, which was a transparent acrylic plate to allow visual inspection. The pin-fin heat sink specimen was located at a distance of 500 mm from the inlet opening.

Int. Journal of Integrated Engineering Vol. 16 No. 6 (2024) p. 100-110

Airflow was controlled by a variable-speed fan at the top of the duct that created negative pressure in the downstream region.

To measure air velocity, an anemometer was positioned at 350 mm from the inlet opening, hence reading the upstream flow. A K-type thermocouple was installed on the upstream (TC_1) and downstream (TC_3) regions as well as on the pin-fin heat sink base plate (TC_2). The heat sink specimen was fitted with a heater at the base plate and power lines were connected to the regulator, voltmeter, and amperemeter to adjust and measure the heater's input electrical power. The schematic and picture of the overall experimental setup are depicted in Figure 1.

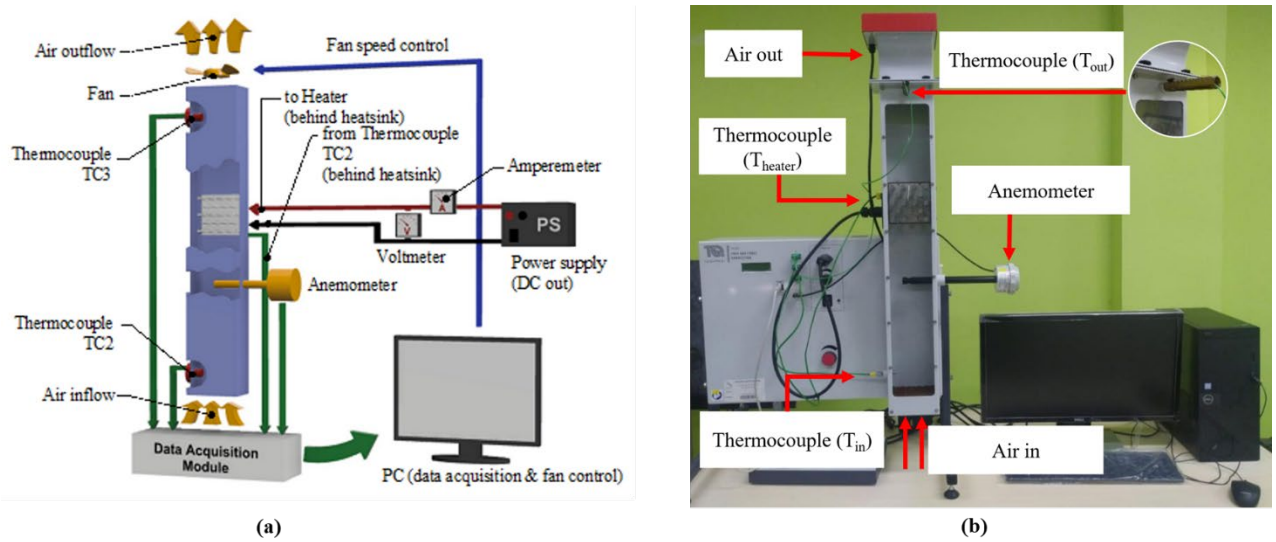

Fig. 1 *Experimental setup (a) Schematics of instrumentation; (b) Forced convection apparatus (TecQuipment TD100) as employed in the laboratory*

A heater and a thermocouple were attached to the back plate to provide a heating effect and measure its temperature. Subsequently, this sub-assembly was stacked together with other components to form the complete heat sink specimen assembly, as seen in Figure 2. A cover at the heater end protected the inner components and wiring and provided insulation to minimize heat loss.

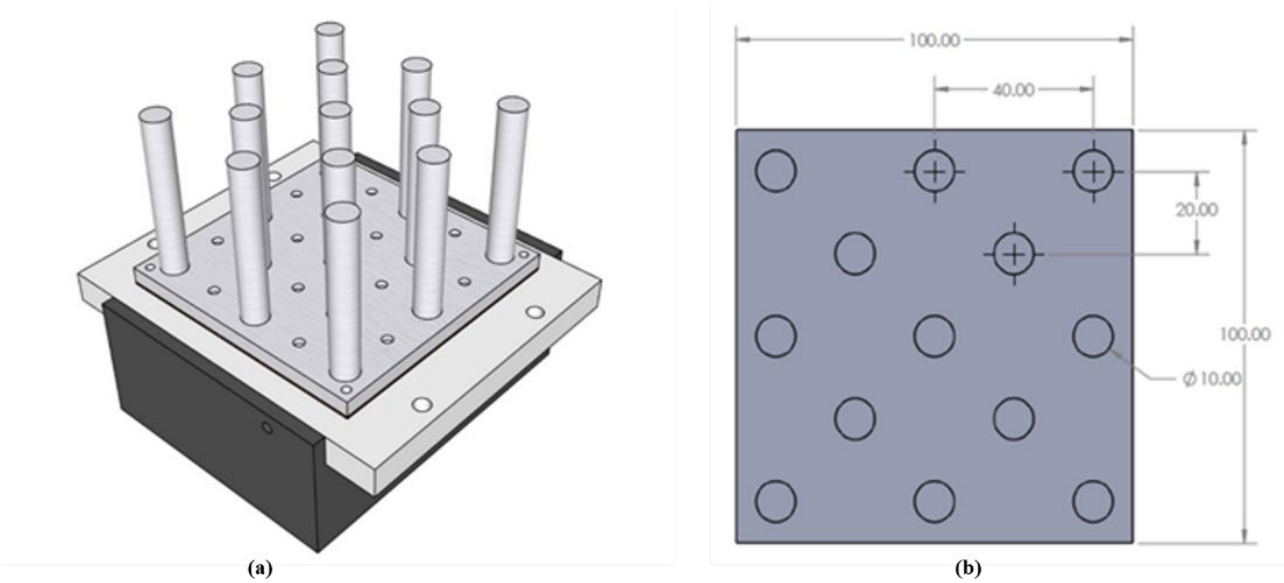

Fig. 2 *Heat sink design (a) Heat sink assembly 3D model; (b) The measurements of pins arrangement Calculations of parameters for performance analysis*

The temperature readings were logged automatically, facilitated by the built-in feature of the TecQuipment TD1005 apparatus called Versatile Data Acquisition System (VDAS). It allowed data acquisition at a certain interval set by the operator upon starting the measurement. In addition, the readings of all three thermocouples are displayed in real-time, therefore the authors were also able to manually record them. This redundancy

(automated data logging and manual recording) provided backup data and at the same time served as a monitoring procedure for the operator to intervene should any anomaly occurred in the process.

Inherently, the heat transfer in this bolted design is not perfect due to the presence of discontinuity on the connections. Among the methods to alleviate this deficiency are applying the thermal paste on interfaces of mating components and ensuring the tightness of bolts. Another consequence of this design is the unused bolt holes, which are exposed to airflow. Nevertheless, as the experiments in this work were made with identical base plates, a number of pins, pin configurations, and assembly techniques, the occurring conditions would also be similar across all experiments. In other words, the authors isolated the variation only to the geometry of pins, keeping the rest of the experimental conditions uniform. Hence results from experiments with different pin geometries can be unambiguously compared.

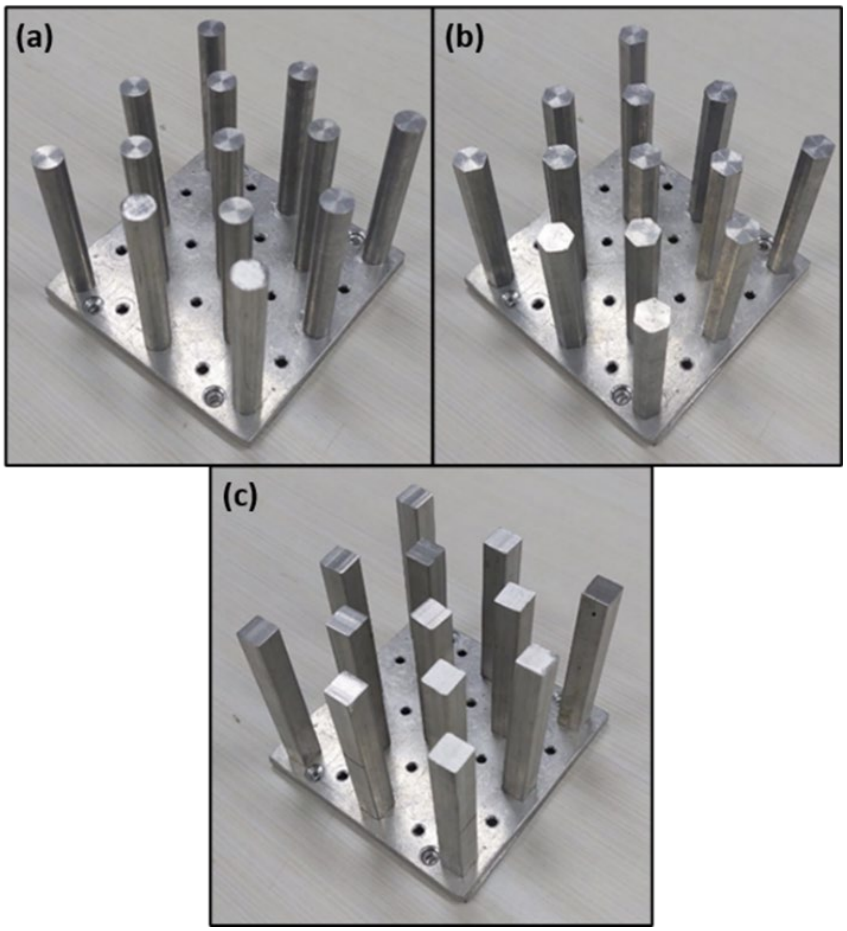

Fig. 3 *Heat sink assembly with different cross-section profile geometry (a) Circular; (b) Hexagonal; and (c) Square*

Three different cross-section geometries of pins, as presented in Figure 3, were used in this research, as mentioned before circular, hexagonal, and square. Those geometries used are among the market's most readily available extruded profiles, hence beneficial from the material sourcing and manufacturing point of view. Cross-sectional sizing of each pin type was based on hydraulic diameter, based on which the Reynolds number calculations were made. The hydraulic diameter was computed using the specimen's dimensional parameters using Equation 1.

$$d_h = \frac{4A}{P} \tag{1}$$

A and P denote the area and perimeter, respectively, of the cross-section. There are 13 pins installed in the heat sink specimen. The dimensional specifications of pins examined in this work are tabulated in Table 1. All pins in the specimen were of aluminum Al-2024. Aluminum is a common heat sink material since it has good thermal conductivity yet is inexpensive as compared to copper, stainless steel, or other higher thermal performance

Int. Journal of Integrated Engineering Vol. 16 No. 6 (2024) p. 100-110

materials. A heater and a thermocouple probe were attached on the back side of the main heat sink assembly. A back cover was also installed to minimize undesired heat loss and protect the components.

Table 1 *Dimensional specifications of pins*

Cross-Sec. Profile	Hyd. Dia. (mm)	S_x/d_h	S_y/d_h	Pin Surf. Area (mm^2)	Pin Vol. (mm^3)
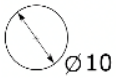	10	4.0	2.0	2199	5498
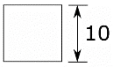	10	4.0	2.0	2800	7000
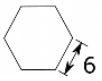	10.4	3.8	1.9	2520	6547

2.2 Calculations of Parameters for Performance Analysis

The heat transfer modes occurring in the investigated system are conduction, convection, and radiation through the air and aluminum. The heat transfer of each mode depends on the temperature of the base plate, assembly material, and the cross-section area of the pin fin. Thus, the heat balance equation for the whole system can be expressed as in Equation 2.

$$Q_{total} = Q_{conv} + Q_{rad} + Q_{loss} \tag{2}$$

In similar studies [29–31], it was reported that the total radiative heat losses from a similar test surface would be about 0.5% of the total electrical heat input. Therefore, the radiative heat loss can be neglected in our case. In this experiment, the heating area was insulated, leading to the assumption of negligible heat loss via conduction. Thus, one can assume that the last two terms of Equation 2 can be zeroed out, resulting in Equation 3.

$$Q_{total} = Q_{conv} \tag{3}$$

The convective thermal resistance of the system can express the ability to release heat from the surface to the environment. This quantity is given by Equation 4 and employed as one of the performance indicators of heat sink geometries investigated in this work. Here, the surrounding temperature is taken by averaging the readings in the inlet and outlet thermocouple ports. Q_{conv}, as discussed in the previous paragraph, is assumed to be equal to the heat supplied by the electric heater.

$$R_{conv} = \frac{((T_{out} + T_{in})/2) - T_h}{Q_{conv}} \tag{4}$$

The steady-state heat transfer from the test section by convection is provided by Equation 5.

$$Q_{conv} = \bar{h} A_T \left[T_h - ((T_{out} + T_{in})/2)\right] \tag{5}$$

Convective heat transfer coefficient, $\bar{h}$, is given by the formula in Equation 6 [32]:

$$\bar{h} = \frac{Q_{conv}}{A_T \left[T_h - ((T_{out} + T_{in})/2)\right]} \tag{6}$$

The convective heat transfer rate, Q_{conv}, is obtained from the electrical input power. Recall that only convective heat transfer is considered since heat transfer associated with radiation and conduction are negligible. T_h, T_{out}, and T_{in} are temperatures of heat sink, outlet air and inlet air, respectively. The overall surface area, A_T is the whole surface of the heat sink in contact with the flowing air, calculated with the formula in Equation 7.

$$A_T = A_{base} + N_f(P \times L) \tag{7}$$

Parameter P is the circumferential length of the pin cross-section, and L is the length of each pin, whose product yields the lateral surface area of one pin. That area of the single pin is multiplied by the number of pins, N_f. For each geometry type, experiments were conducted at a heater input power of 15 W and 20 W. The experiments were done at varied air velocities of 1 m/s, 1.5 m/s, 2 m/s, and 2.5 m/s, measured at the upstream section. Those velocity values were then translated into Reynolds numbers via Equation 8.

$$\mathrm{Re}_D = \frac{U_{pin} d_h}{\nu_{air}} \tag{8}$$

In calculating the Reynolds number, vair denotes the kinematic viscosity of air, while dh is obtained from Equation 1. This Reynolds number is based on the flow condition around pins. Thus, the characteristic length taken here is the pin hydraulic diameter. Likewise, the velocity used occurs in the vicinity of the pins instead of that in the free stream region as measured by the anemometer. Thus, to obtain the velocity of air in the vicinity of the pins, continuity relation is applied to give Equation 9.

$$U_{pin} = \left(\frac{A}{A - A_{front}} \right) U \tag{9}$$

There, A is the cross-sectional duct area away from the test section, 9600 mm2, according to the specification as mentioned before. The front is the frontal area of first-row pins that protrude into the airflow column. Heat transfer characteristics can also be described by the Nusselt number. It describes the ratio of heat transfer by conduction and convection, given by Equation 10. The thermal conductivity of air, k, varies with temperature based on the table in a book by Incropera-DeWitt [33]. However, since the value of k only experiences minute change within our experimental temperature range, then Nu directly follows the h.

$$Nu = \frac{\bar{h} d_h}{k} \tag{10}$$

3. Results from Experiments and Analytical Approach

3.1 Heatsink Temperature

The temperature at the base of the heat sink represents that of the heat source. In the case of electronic applications, it can be any heat-producing components such as resistors, processors, etc. In Figure 4, the heat sink temperature is plotted against the inlet air velocity for each pin geometry. All the data points were obtained from the apparatus' automatic data logger, which values were identical with those recorded manually, hence verifying the accuracy. The data was cleaned and processed in a spreadsheet (Microsoft Excel), then the graphs/plots were generated in a separate graphing software (Origin).

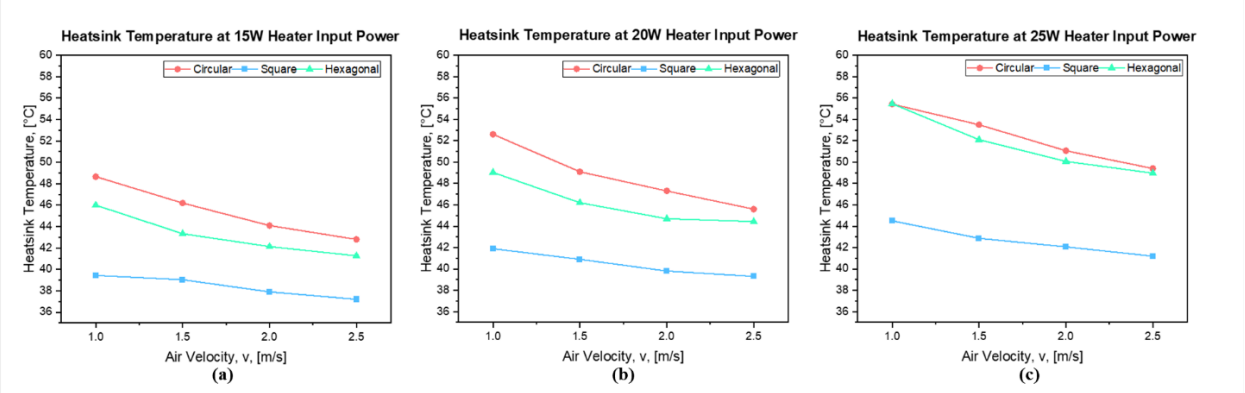

Int. Journal of Integrated Engineering Vol. 16 No. 6 (2024) p. 100-110

Fig. 4 *Heat sink surface temperature under different inlet airflow velocities at 3 variations of heater input power (a) 15 W; (b) 20 W; and (c) 25 W*

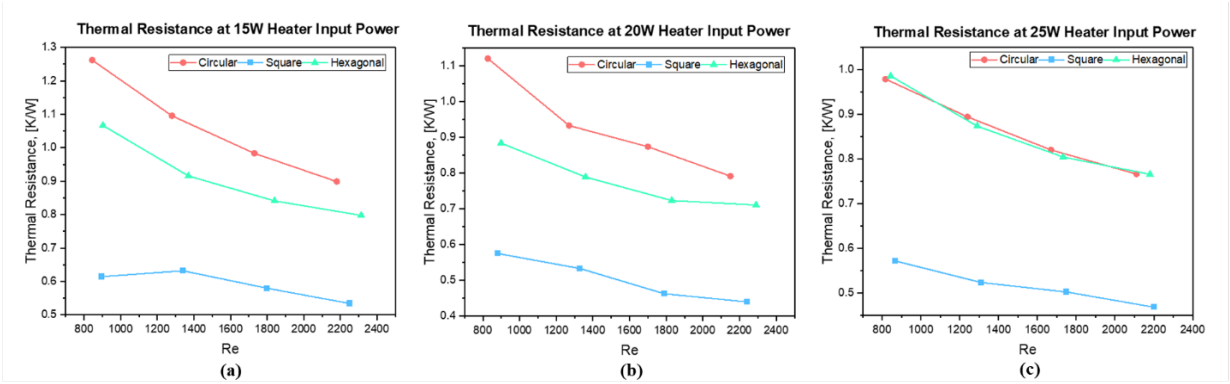

Fig. 5 *Thermal resistance decreases with the Reynolds number that reflects the airflow velocity (a) 15 W; (b) 20 W; and (c) 25 W*

With our setup, consistent results have been obtained in heat sink base temperature, where the square fin demonstrates excellent performance for the same hydraulic diameter compared to the other tested geometries in maintaining a low heat sink temperature. However, this excellence is achieved at the expense of the material volume, as in Table 1, where a square pin has the largest volume for a given hydraulic diameter, followed by hexagonal and circular shapes.

In addition to observing surface temperature, the thermal resistance of each geometry is also assessed. Thermal resistance is a function of the temperature gradient between the heat sink surface and ambient temperature. This parameter is important because the temperature of the heat sink itself depends on the ambient temperature, which may fluctuate during experiments. In our experiments, inlet temperature was maintained at 29°C +/- 0.7°C. It turns out that the presence of temperature fluctuation in our experiments, as seen in Figure 5, does not significantly change the order of performance, except that in 25 W input power, the hexagonal and circular pin graphs coincide. Overall, the thermal resistance drops at higher Reynolds numbers. The order of the cooling performance as observed in the graphs in Figures 4 and 5 can also be related to the surface area of pin geometries. Nonetheless, the relation between the resulting temperature difference and fin surface area is not trivial. For instance, the surface area of the hexagonal pin is 15% larger than the circular one, and it yields a 14% lower temperature gradient in the experiment using 15 W heater input power.

On the other hand, a square pin with 27% larger surface area than a circular pin creates 42% lower temperature gradient. A more prominent phenomenon is shown in the 25 W heater power, where the difference between hexagonal and circular geometries becomes negligible. Meanwhile, the square shape can produce 38% lower temperature gradient than the others.

3.2 Heat Transfer

The performance of each pin geometry in terms of heat transfer is described in the below graphs of the convective heat transfer coefficient. As one can infer from the previous temperature-related discussions, the heat transfer parameters calculations show that square geometry yields the highest coefficients compared to the other tested geometries. The explanation for this finding is that the square cross-section creates a turbulent field that intensifies interactions between fluid flow wake and the adjacent surfaces, hence increasing heat transfer [34]. Circular and hexagonal pins show heat transfer performances that are close to each other. Still, despite having a narrow difference in heat transfer coefficients, the hexagonal pin-fin is capable of maintaining a lower heat sink temperature than the circular counterpart (see Figure 6) due to its larger surface area.

The obtained results are in a good agreement with the previous works of other investigators that demonstrate the superiority of square pin geometry over the circular one in terms of heat transfer characteristics [35]. As for the hexagonal geometry, published works show contradicting conclusions on its heat transfer performance compared to other shapes, where some investigations show higher coefficients and others demonstrate the opposite [36]. Another observation from the experiment is that the heat transfer coefficient tends to increase with surface temperature at a given air inlet velocity. In Figure 7, the trendline is obtained by linear regression of 3 data points for each geometry, where each point is a result of averaging 3 data from experiments at different input powers: 15 W, 20 W, 25 W. This characteristic was also encountered by former investigator [37] who observed the increase of heat transfer coefficient as surface temperature goes up in a jet impinging experiment with variation in surface temperature.

Figure 6 shows the variation of the heat transfer coefficient with heat sink base temperature at 4 different inlet velocity cases (1, 1.5, 2, and 2.5 m/s). By looking at the linear fitting line for each geometry at each inlet velocity case, one can infer that the heat transfer coefficient of a heat sink gets higher as its temperature rises. This result can be further refined and verified by acquiring a larger amount of data points using more variations of heater input power settings.

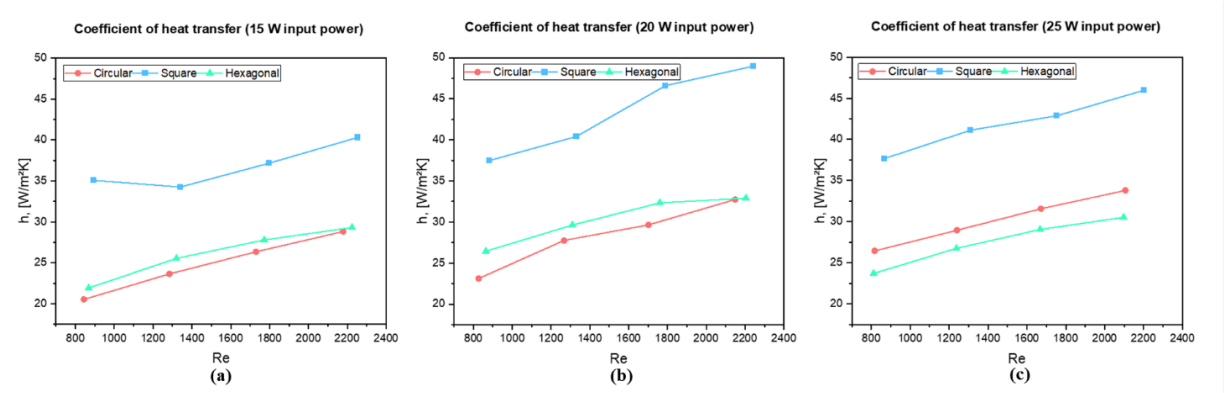

Fig. 6 *All test conditions share similar characteristics: coefficient of convective heat transfer raises with Reynolds number (a) 15 W; (b) 20 W; and (c) 25 W*

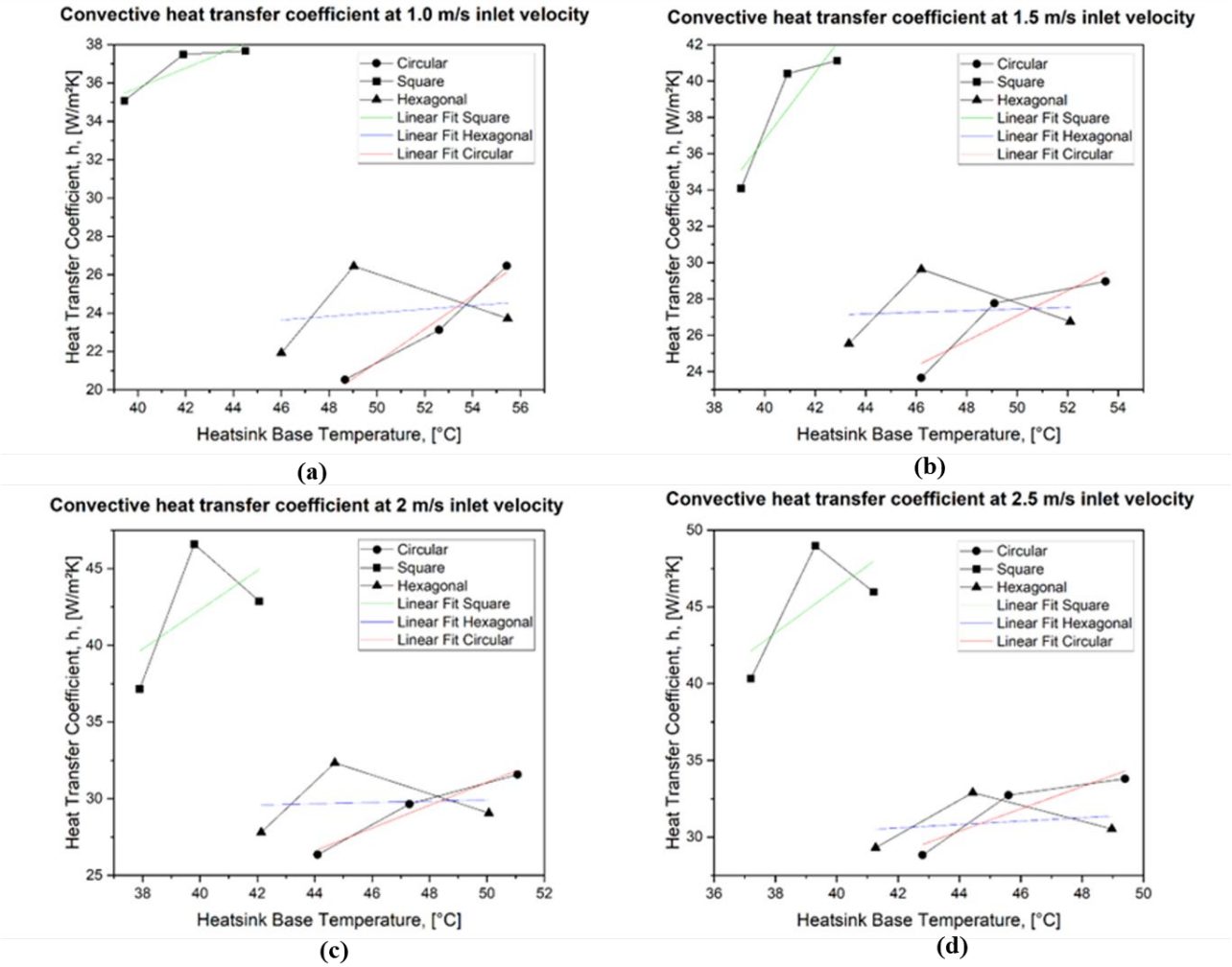

Fig. 7 *Linear regression lines show that the heat transfer coefficient increases with surface temperature*

4. Conclusion

Through this work, authors have demonstrated the use of a modular pin-fin heat sink specimen for investigating the characteristics of different pin geometries. Experimental results obtained with this device have shown a good

agreement with those shown in various published works, therefore implying their validity. The data from experiments with all pin shapes confirm the a priori knowledge that heat transfer increases with the velocity of the fluid, causing lower heat sink surface temperature. Heat sink with square pins shows superiority over circular and hexagonal counterparts in its ability to dissipate heat. The ease of manufacturing processes goes alongside heat transfer performance to justify the advantage of using square pins.

An important remark for this work is that the results of this work are obtained with uniform hydraulic diameters for all pin shapes. It is intended to acieve the same Reynolds regime when they are blown by air at the same flow velocity. Nevertheless, the downside is that the same hydraulic diameter leads to a different surface area which intuitively affects the heat transfer rate. Future works will cover this issue to verify the findings reported in this paper. The planned experiments are to compare pins of the same surface area instead of hydraulic diameters. Thus, adjusting flow velocities settings for each shape is required to keep the flow in the same Reynolds regime for all cases. Additionally, a comparison with a commercial heatsink of similar dimension at the same heat emission is an important part of the upcoming works, since it will link this research outcomes with the real industrial practices. That comparison remains valuable despite the common commercial use of square or rectangular pin geometry due to the manufacturing feasibility, which geometry has also been shown in this report for exhibiting superior performance as compared to circular and hexagonal ones.

Acknowledgement

Our appreciation extends to our colleagues in the Integrated Laboratory Unit of Institut Teknologi Sumatera, Indonesia, who have given us access to various measurement tools and working space.

Conflict of Interest

Authors declare that there is no conflict of interests regarding the publication of the paper.

Author Contribution

The authors confirm contribution to the paper as follows: ***conceptualization, formal analysis, validation, original draft writing:*** *Devia Gahana Cindi Alfian;* ***methodology, visualization, writing-review & editing:*** *Dicky Januarizky Silitonga;* ***data collection:*** *Muhammad Al Fajri Ramadhan, Ihsan Naufal Ridhwan;* ***investigation:*** *Rionaldi Prasetyo Utomo, I Made Rudiarta. All authors reviewed the results and approved the final version of the manuscript.*

References

[1] Yang, H., Li, Y., Zhang, L. & Zhu, Y. (2021). Thermal performance enhancement of phase change material heat sinks for thermal management of electronic devices under constant and intermittent power loads. International Journal of Heat and Mass Transfer, 181. https://doi.org/10.1016/j.ijheatmasstransfer.2021.121899

[2] He, Z., Yan, Y. & Zhang, Z. (2021). Thermal management and temperature uniformity enhancement of electronic devices by micro heat sinks: A review. Energy, 216. https://doi.org/10.1016/j.energy.2020.119223

[3] Di Capua H, M. & Jahn, W. (2021). Performance assessment of thermoelectric self-cooling systems for electronic devices. Applied Thermal Engineering, 193. https://doi.org/10.1016/j.applthermaleng.2021.117020

[4] Su, G., Liao, T., Chen, L. & Chen, J. (2016). Performance evaluation and optimum design of a new-type electronic cooling device. Energy, 101, pp. 421–426. https://doi.org/10.1016/j.energy.2016.02.059

[5] Arshad, A., Ibrahim Alabdullatif, M., Jabbal, M. & Yan, Y. (2021). Towards the thermal management of electronic devices: A parametric investigation of finned heat sink filled with PCM. International Communications in Heat and Mass Transfer, 129. https://doi.org/10.1016/j.icheatmasstransfer.2021.105643

[6] Rani, J. R., Das, N. C., Kim, M. & Jang, J. H. (2022). Low-temperature characteristics of resistive switching memory devices based on reduced graphene oxide-phosphor composites toward reliable cryogenic electronic devices. Carbon, 195, pp. 174–182. https://doi.org/10.1016/j.carbon.2022.04.016

[7] Toosi, M. H. & Siavashi, M. (2017). Two-phase mixture numerical simulation of natural convection of nanofluid flow in a cavity partially filled with porous media to enhance heat transfer. Journal of Molecular Liquids, 238, pp. 553–569. https://doi.org/10.1016/j.molliq.2017.05.015

[8] Tao, D. et al. (2021). Heat transfer evaluation of natural convection outside the condenser in Passive Residual Heat Removal System of Molten Salt Reactor. Case Studies in Thermal Engineering, 28. https://doi.org/10.1016/j.csite.2021.101611

[9] Colombo, M. & Fairweather, M. (2021). Study of nuclear reactor external vessel passive cooling using computational fluid dynamics. Nuclear Engineering and Design, 378. https://doi.org/10.1016/j.nucengdes.2021.111186
[10] Qin, P., Liao, M., Mei, W., Sun, J. & Wang, Q. (2021). The experimental and numerical investigation on a hybrid battery thermal management system based on forced-air convection and internal finned structure. Applied Thermal Engineering, 195. https://doi.org/10.1016/j.applthermaleng.2021.117212
[11] Lyu, C. et al. (2021). A new structure optimization method for forced air-cooling system based on the simplified multi-physics model. Applied Thermal Engineering, 198. https://doi.org/10.1016/j.applthermaleng.2021.117455
[12] Hnayno, M. et al. (2022). Performance analysis of new liquid cooling topology and its impact on data centres. Applied Thermal Engineering, 213, pp. 118733. https://doi.org/10.1016/j.applthermaleng.2022.118733
[13] Samudre, P. & Kailas, S. V. (2022). Thermal performance enhancement in open-pore metal foam and foam-fin heat sinks for electronics cooling. Applied Thermal Engineering, 205. https://doi.org/10.1016/j.applthermaleng.2021.117885
[14] Khattak, Z. & Ali, H. M. (2019). Air cooled heat sink geometries subjected to forced flow: A critical review. International Journal of Heat and Mass Transfer, 130, 141–161. https://doi.org/10.1016/j.ijheatmasstransfer.2018.08.048
[15] Zhang, D., Fu, L., Guan, J., Shen, C. & Tang, S. (2022). Investigation on the heat transfer and energy-saving performance of microchannel with cavities and extended surface. International Journal of Heat and Mass Transfer, 189. https://doi.org/10.1016/j.ijheatmasstransfer.2022.122712
[16] Huang, L., Li, Q. & Zhai, H. (2018). Experimental study of heat transfer performance of a tube with different shaped pin fins. Applied Thermal Engineering, 129, 1325–1332. https://doi.org/10.1016/j.applthermaleng.2017.10.014
[17] Hussain, A. A., Freegah, B., Khalaf, B. S. & Towsyfyan, H. (2019). Numerical investigation of heat transfer enhancement in plate-fin heat sinks: Effect of flow direction and fillet profile. Case Studies in Thermal Engineering, 13. https://doi.org/10.1016/j.csite.2018.100388
[18] Liu, X., Yu, J. & Yan, G. (2016). A numerical study on the air-side heat transfer of perforated finned-tube heat exchangers with large fin pitches. International Journal of Heat and Mass Transfer, 100, 199–207. https://doi.org/10.1016/j.ijheatmasstransfer.2016.04.081
[19] Zhang, C. N. & Li, X. F. (2020). Temperature distribution of conductive-convective-radiative fins with temperature-dependent thermal conductivity. International Communications in Heat and Mass Transfer, 117. https://doi.org/10.1016/j.icheatmasstransfer.2020.104799
[20] Paidar, M. et al. (2022). The influence of the backing plate materials on microstructure and mechanical properties of friction spot extrusion brazing of AA2024-T3 aluminum alloy and Brass sheets. Journal of Manufacturing Processes, 74, 28–39. https://doi.org/10.1016/j.jmapro.2021.12.002
[21] Muhammad, E. H. (2013). A Comparison of the Heat Transfer Performance of a Hexagonal Pin Fin with Other Types of Pin Fin Heat Sinks, International Journal of Science and Research vol. 4 www.ijsr.net
[22] Kanyakam, S. & Bureerat, S. (2011). Multiobjective evolutionary optimization of splayed pin-fin heat sink. Engineering Applications of Computational Fluid Mechanics, 5, 553–565. https://doi.org/10.1080/19942060.2011.11015394
[23] Keyes, R. W. (1984). Heat Transfer in Forced Convection Through Fins. IEEE Transactions on Electron Devices, 31, 1218–1221. https://doi.org/10.1109/T-ED.1984.21691
[24] Annuar, K. A. M. & Ismail, F. S. (2014). Optimal pin fin arrangement of heat sink design and thermal analysis for central processing unit, in 2014 5th International Conference on Intelligent and Advanced Systems: Technological Convergence for Sustainable Future, ICIAS 2014 - Proceedings (IEEE Computer Society, 2014). https://doi.org/10.1109/ICIAS.2014.6869537
[25] Jin, W. et al. (2021). Effect of shape and distribution of pin-fins on the flow and heat transfer characteristics in the rectangular cooling channel. International Journal of Thermal Sciences, 161. https://doi.org/10.1016/j.ijthermalsci.2020.106758
[26] Lyall, M. E., Thrift, A. A., Kohli, A. & Thole, K. A. (2007). Heat transfer from low aspect ratio pin fins, in Proceedings of the ASME Turbo Expo, 4, 413–422. https://doi.org/10.1115/GT2007-27431
[27] Ghisalberti, L. & Kondjoyan, (1999). A. Convective heat transfer coeficients between air flow and a short cylinder. Efect of air velocity and turbulence. Efect of body shape, dimensions and position in the flow, www.elsevier.com/locate/jfoodeng
[28] Ambreen, T. & Kim, M. H. (2018). Effect of fin shape on the thermal performance of nanofluid-cooled micro pin-fin heat sinks. International Journal of Heat and Mass Transfer, 126, 245–256. https://doi.org/10.1016/j.ijheatmasstransfer.2018.05.164
[29] Naik, S., Probert, S. D. & Shilston, M. J. (1987). Forced-Convective Steady-State Heat Transfers from Shrouded Vertical Fin Arrays, Aligned Parallel to an Undisturbed Air-Stream, Applied Energy, 26.

[30] Hwang, J.-J. & Liou, T.-M. (1998). Heat Transfer and Friction in a Low-Aspect-Ratio Rectangular Channel with Staggered Slit-Ribbed Walls*, International Journal of Rotating Machinery, 4.
[31] El-Sayed, S. A., Mohamed, S. M., Abdel-Latif, A. M. & Abouda, A.-H. E. (2002). Investigation of turbulent heat transfer and fluid flow in longitudinal rectangular-fin arrays of different geometries and shrouded fin array, www.elsevier.com/locate/etfs.
[32] Cattani, L., Maillet, D., Bozzoli, F. & Rainieri, S. (2015). Estimation of the local convective heat transfer coefficient in pipe flow using a 2D thermal Quadrupole model and Truncated Singular Value Decomposition. International Journal of Heat and Mass Transfer, 91,1034–1045. https://doi.org/10.1016/j.ijheatmasstransfer.2015.08.016
[33] Bergman, T. L., Lavine, A. S., Incropera, F. P. & DeWitt, D. P. (2011). Fundamentals of Heat and Mass Transfer 7th edition", John Wiley & Sons, pp. 1–1076, 2011.
[34] Liou, T. M., Chen, S. H. & Hwang, P. W. (2002). Large eddy simulation of turbulent wake behind a square cylinder with a nearby wall", Journal of Fluids Engineering, Transactions of the ASME, 124, 81–90. https://doi.org/10.1115/1.1445797
[35] Ambreen, T., Saleem, A. & Park, C. W. (2019). Pin-fin shape-dependent heat transfer and fluid flow characteristics of water- and nanofluid-cooled micropin-fin heat sinks: Square, circular and triangular fin cross-sections. Applied Thermal Engineering, 158. https://doi.org/10.1016/j.applthermaleng.2019.113781
[36] Zhang, J., Han, H. Z., Li, Z. R. & Zhong, H. G. (2021). Effect of pin-fin forms on flow and cooling characteristics of three-layer porous laminate. Applied Thermal Engineering, 194. https://doi.org/10.1016/j.applthermaleng.2021.117084
[37] Ndao, S., Peles, Y. & Jensen, M. K. (2014). Effects of pin fin shape and configuration on the single-phase heat transfer characteristics of jet impingement on micro pin fins. International Journal of Heat and Mass Transfer, 70, pp. 856–863. https://doi.org/10.1016/j.ijheatmasstransfer.2013.11.062